

Strain Rate Effects on the Behavior of
Shape Memory Alloys

by

Amanda Olender

Submitted to the
Department of Materials Science and Engineering
in Partial Fulfillment of the Requirements for the Degree of
Bachelor of Science

at the

Massachusetts Institute of Technology

June 2013

© 2013 Amanda Olender
All Rights Reserved

The author hereby grants to MIT permission to reproduce
and to distribute publicly paper and electronic copies of this thesis document
in whole or in part in any medium now known or hereafter created.

Signature of Author

Department of Materials Science and Engineering
May 10, 2013

Certified by

Christopher A. Schuh
Department Head of Materials Science and Engineering
Thesis Supervisor

Accepted by

Jeffrey C. Grossman
Carl Richard Soderberg Associate Professor of Power Engineering
Chair, Undergraduate Thesis Committee

Strain Rate Effects on the Behavior of Shape Memory Alloys

by

Amanda Olender

Submitted to the Department of Materials Science and Engineering
on May 10, 2013 in Partial Fulfillment of the Requirements for
the Degree of Bachelor of Science in Materials Science and Engineering

ABSTRACT

Shape memory alloys are a unique category of metals characterized by a solid phase transformation between austenite and martensite when exposed to either a thermal or physical external stress. This allows for recovery of the original shape of the material when the stress is removed. Cu-based SMAs have recently grown in popularity due to their lower cost, easier fabrication, and higher working temperatures than the currently used Ni-Ti alloys. This research investigates the pseudoelastic properties of Cu-Al-Mn-Ni oligocrystalline wires that have the potential to be used in SMA applications.

Various factors affecting the pseudoelastic hysteresis were investigated, including strain rate, grain size, and electropolishing conditions. It was found that increasing strain rate decreases the size of the hysteresis, and that for wire diameters above 100 μm , no correlation exists between wire size and pseudoelastic transformation stresses. Electropolishing until a smooth surface texture was achieved was determined to be beneficial to the pseudoelastic response of the wire, but overpolishing had detrimental effects.

Thesis Supervisor: Christopher A. Schuh

Title: Department Head of Materials Science and Engineering

Table of Contents

LIST OF TABLES	4
LIST OF FIGURES	4
1. INTRODUCTION	5
1.1 Current alloys.....	7
1.2 Microstructure.....	9
1.3 Pseudoelastic hysteresis	11
1.4 Factors affecting the hysteresis	12
1.4.1 Strain rate	12
1.4.2 Wire diameter.....	13
1.4.3 Surface texture	14
1.4.4 Training.....	14
2. METHODOLOGY	15
2.1 Preparing wires	15
2.2 Finding transformation temperatures	17
2.3 Testing pseudoelasticity	19
3. RESULTS AND DISCUSSION	20
3.1 Composition effects	20
3.2 Strain rate effects	21
3.3 Wire diameter effects.....	23
3.4 Surface texture effects.....	24
4. CONCLUSION.....	26
5. FUTURE WORK.....	27
6. ACKNOWLEDGEMENTS	28
7. BIBLIOGRAPHY	29

LIST OF TABLES

Table 1. Wire details, including composition, diameter, and polishing details.	17
Table 2. Compositions and transformation temperatures of the wires used by Sari.	18
Table 3. Transformation stresses σ_{Ms} and σ_{As} for Wire B (D=98 μ m) for various load rates.	22

LIST OF FIGURES

Figure 1. Temperature and stress dependence of shape memory and pseudoelasticity	6
Figure 2. Schematic of shape memory and pseudelastic hystereses	7
Figure 3. Vertical section of Cu-Al-10%Mn phase diagram	9
Figure 4. SEM images of Wire C and Wire F.....	16
Figure 5. Thermal cycling data for Sample C at a constant load of 20 MPa	18
Figure 6. Pseudoelastic hystereses for Wire A (Cu-Al-Mn) and Wire B (Cu-Al-Mn-Ni).....	20
Figure 7. Pseudoelastic hysteresis for Wire B (D=98 μ m) at various strain rates	21
Figure 8. Pseudoelastic hystereses for Cu-Al-Mn-Ni wires of varying diameters.....	23
Figure 9. Relationship between σ_{Ms} and wire diameter	24
Figure 10. SEM images of Wire F as-pulled and after electropolishing.....	25
Figure 11. SEM images of Wire H as-pulled and after electropolishing	25

1. INTRODUCTION

Shape memory alloys (SMAs) are metals that have significant strain recovery after being thermally or physically stressed. A solid-state phase transition occurs in the material between the austenite and martensite crystal structures, which allows for this phenomenon. The transition happens through the classic nucleation and growth process, where unique martensite clusters develop and grow within each grain (Zhang, Feng, He, Yu, & Sun, 2010). From an energy standpoint, there is a gradient term in the free energy, so even if the wire is at a local energy minimum, the transformation will continue to occur until the entire wire has changed phases (Grandi, Maraldi, & Molari, 2012). If the driving force is temperature, the transformation process is known as the shape memory effect (SME). For a driving force of external stress, the process is called pseudoelasticity.

The responses of SMAs to temperature and external stress are inherently linked. As shown in Figure 1, as the temperature increases, the transition stresses also increase. Similarly, an increase in initial stress causes the transition temperatures to rise. For small wires, especially at high strain rates, internally generated heat must also be considered. The A→M transition is exothermic, so the material self-heats, which may cause the A→M transition temperatures to rise. Conversely, the M→A transition is endothermic, so the material temperature drops and the M→A temperatures decrease (Grandi, Maraldi, & Molari, 2012). However, as the wire diameter increases above 120 μm , latent heat effects are minimized as the heat can dissipate faster than it can be absorbed into the wire (Lopez del Castillo, Mellor, Blazquez, & Gomez, 1987).

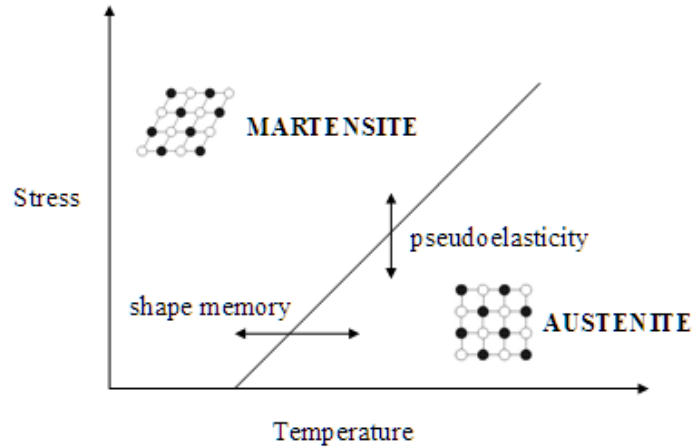


Figure 1. The relationship between temperature and stress for shape memory and pseudoelastic transformations.

Because austenite is a more ordered phase than martensite, the sample expands during the A→M transition. This causes a positive strain to develop, a large percentage of which, due to the unique property of SMAs, can be recovered during the M→A transition, though there is significant energy loss during the process. Thus, when an SMA is subjected to thermal or stress cycles, a strain-temperature or stress-strain hysteresis results, respectively. From this hysteresis, it is possible to discern the transition temperatures (martensite start, M_s ; martensite finish, M_f ; austenite start, A_s ; austenite finish, A_f) and stresses (martensite start, σ_{M_s} ; martensite finish, σ_{M_f} ; austenite start, σ_{A_s} ; austenite finish, σ_{A_f}). Figure 2 shows schematics of the hystereses for both shape memory and pseudoelasticity and the respective locations of the transition temperatures and stresses along the hystereses.

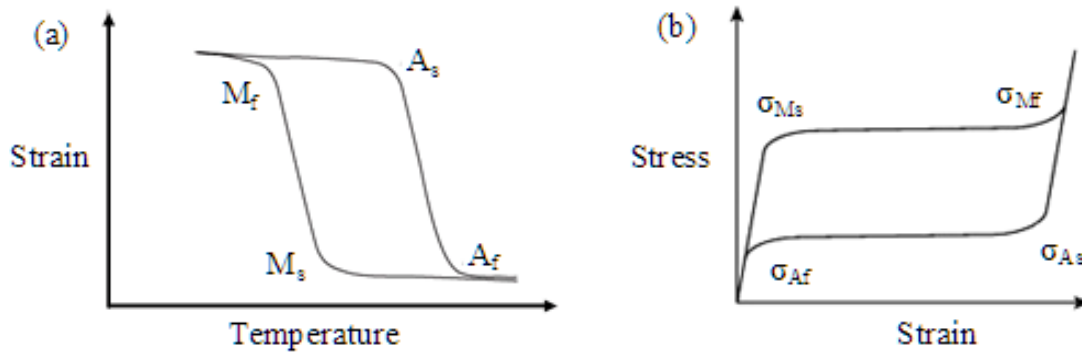


Figure 2. (a) Schematic of shape memory hysteresis.
 (b) Schematic of pseudoelasticity hysteresis.

The amount of energy absorbed during the cycle is defined as the area contained within the hysteresis (see Section 1.3 Pseudoelastic hysteresis). Thus many applications for SMAs involve energy damping, including force actuation devices, impact absorption, and energy conversion. Additionally, SMAs have been used as coupling mechanisms and in smart microdevices (Davis & Associates, 2001) (Chen & Schuh, 2011).

1.1 Current alloys

One currently popular SMA is Nitinol, an alloy of nickel and titanium in approximately equal atomic percents. This alloy has an austenite finish temperature $A_f < 50^\circ\text{C}$, which allows its use in many room temperature applications, including orthodontics and structural engineering projects (Ren, Bai, Wang, Zheng, & Li, 2008) (Chen, et al., 2006). However, Ni-Ti SMAs are difficult and expensive to produce, and their low transition temperatures do not allow for high

temperature ($>100^{\circ}\text{C}$) applications (Tobushi, Shimeno, Hachisuka, & Tanaka, 1998). Thus there is currently a great deal of ongoing research on Cu-based alloys as a cheaper, easier to produce, and higher temperature alternative to Ni-Ti alloys (Lopez del Castillo, Mellor, Blazquez, & Gomez, 1987) (Sari, 2010).

Cu-Al-Ni and Cu-Zn-Al are two promising alloys for new SMAs. The Cu-Al-Ni alloys that have shape memory properties include 11-14.5% Al and 3-5% Ni, with the balance Cu (composition percentages are in weight percent, unless otherwise specified) (Sari, 2010). The major concern with these alloys, however, is that they are brittle and are susceptible to intergranular cracks (Omori, Koeda, Sutou, Kainuma, & Ishida, 2007) (Sari, 2010). Thus other alloys, specifically Cu-Al-Mn, have also been investigated.

Sutou et. al. found that Cu-Al-Mn alloys with less than 18% Al show good SME and have a much higher ductility than Cu-Al-Ni SMAs during phase transitions. However, the total pseudoelastic strain is limited to under 2% instead of the 8% that can be achieved with Cu-Zn-Al and almost 10% that is possible with Cu-Al-Ni (Sutou, Omori, Kainuma, Ono, & Ishida, 2002) (Ueland & Schuh, 2012) (Otuska, Wayman, Nakai, Sakamoto, & Shimizu, 1976). Thus in order to get the good strain rates of Cu-Al-Ni and the ductility of Cu-Al-Mn, recent research has suggested that Cu-Al-Mn-Ni is a good candidate for SMA applications (Omori, Koeda, Sutou, Kainuma, & Ishida, 2007) (Sari, 2010). Sari has shown that a 2.5% Mn addition to Cu-11.9% Al-3.8% Ni results in a 75% grain size reduction, which in turn improves the ductility from 8% to 15% due the reduction of potential intergranular fracture (Sari, 2010). Because there is relatively little literature on Cu-Al-Mn-Ni SMAs, this research seeks to study this alloy in more detail and compare it to the results reported in the literature as well as the behavior of other SMAs.

1.2 Microstructure

The shape memory effect results from a reversible austenite to martensite phase transition. For Cu-Al-Ni alloys, this means a transition between the β_1 (austenite) and β'_1 (low Al martensite) + γ'_1 (high Al martensite) phases. The addition of Mn stabilizes just the β'_1 phase at low temperatures. This phase has better thermoelastic behavior than γ'_1 , so the Mn addition improves the overall properties of the alloy (Sari, 2010). Additionally, the addition of Mn increases the allowable variation in composition for which SME is found (Omori, Koeda, Sutou, Kainuma, & Ishida, 2007). The applicable region of the Cu-10at%Mn-Al phase diagram is shown in Figure 3. To lock in the high temperature β structure at room temperature, it must be heat treated above 600-800°C, depending on the composition, and then subsequently quenched in water.

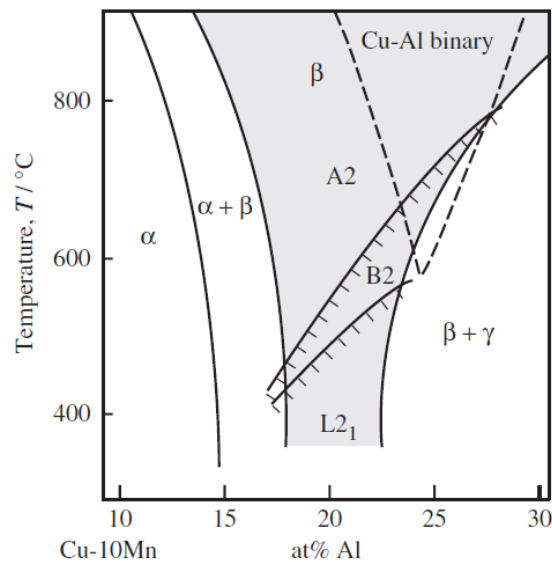


Figure 3. Vertical section of Cu-Al-10%Mn phase diagram with β phase of Cu-Al binary system indicated by broken line. Source: (Omori, Koeda, Sutou, Kainuma, & Ishida, 2007).

The A→M transition that occurs as a result of heating or induced stress follows a nucleation and growth pattern of martensitic plates. Nucleation sites can occur both along grain boundaries as well as within grains themselves. Because of the volume change during the transition, friction between grains and free surfaces resists the growth of the martensitic plates (Ueland & Schuh, 2012) (Chen & Schuh, 2011). Thus the driving force, whether thermal or physical, must increase to overcome this additional energy barrier for interface propagation to occur. If this frictional energy is large enough, the transition stresses may become greater than the yield strength of the material so the material may fail before any SME is shown. Therefore, one way to reduce the pinning force is to increase the total free surface area to grain boundary ratio, one way of which is through oligocrystalline structures (Ueland & Schuh, 2012).

Oligocrystalline structures, defined as those in which the total surface area is greater than the total grain boundary area, include bamboo-structured fine wires and open-cell foams. Bamboo-structured wires in particular are ideal for SMAs also because they reduce, and ideally eliminate, triple junctions that are the main cause of failure in these materials. Polycrystalline SMAs show much lower strain recovery than single crystals, so having a bamboo structure gives wires the ability to reach the high strain recovery of single crystals while making the processing of the wires much easier and less expensive than that for single crystals. Ueland, Chen, and Schuh showed that a perfect oligocrystal can reach almost 7% strain that is completely reversible, compared to the 10% reversible strain for single crystals (Ueland, Chen, & Schuh, 2012) (Otuska, Wayman, Nakai, Sakamoto, & Shimizu, 1976). Polycrystals, on the other hand, can only reach an irreversible 4% strain before fracture occurs (Sakamoto, Kijima, & Shimizu, 1982). As a result, this research will look at the shape memory capabilities of oligocrystalline wires.

1.3 Pseudoelastic hysteresis

In this research, pseudoelastic behavior of Cu-Al-Mn-Ni wires is investigated. The hysteresis formed during stress-induced cycles is thus of importance. (See Figure 2(b) for a schematic of the hysteresis.) From the hysteresis, transformation stresses, energy dissipation, and recoverable strain energy can all be determined. The locations of the transformation stresses (σ_{Ms} , σ_{Mf} , σ_{As} , σ_{Af}) are depicted in Figure 2(b). The energy dissipated, E_d , during the phase transformations is defined by the area enclosed by the loading and unloading curves (Eq. 1) (Tobushi, Shimeno, Hachisuka, & Tanaka, 1998).

$$E_d = (\sigma_{Ms} - \sigma_{As})\epsilon_{Ms} \quad \text{Eq. 1}$$

The recoverable strain energy per unit volume, E_r , is the area below the unloading curve (Eq. 2, where E is the Young's modulus) (Tobushi, Shimeno, Hachisuka, & Tanaka, 1998).

$$E_r = \sigma_{As}\epsilon_{As} + \sigma_{Ms}^2/2E \quad \text{Eq. 2}$$

Chen and Schuh investigated strain energy, and determined that one way to compare the energy dissipation between different wires was to normalize the area within the hysteresis by the maximum strain reached, which they called $\Delta E_{1\%}$, or the characteristic strain energy dissipation per unit strain. They also determined that there was a linear relationship between $\Delta E_{1\%}$ and $\Delta\sigma$, where $\Delta\sigma$ is defined in Eq. 3. Therefore, $\Delta\sigma$ can be used as a measure of the energy dissipation capacity of a wire.

$$\Delta\sigma = \frac{\sigma_{Ms} + \sigma_{Mf}}{2} - \frac{\sigma_{As} + \sigma_{Af}}{2} \quad \text{Eq. 3}$$

The slopes of both the initial loading before σ_{Ms} is reached as well as that of the plateau during the martensitic transformation (σ_{Ms} through σ_{Mf}) are the result of a combination of thermal and mechanical effects (Grandi, Maraldi, & Molari, 2012). Wires are tested above A_f so they start at and return fully to austenite between cycles. This high temperature promotes the stability of the austenite phase, even while it is mechanically deformed. As the testing temperature increases, then, σ_{Ms} also increases. One major caution to this is that if the testing temperature is too far above A_f , σ_{Mf} may exceed the yield stress of the material. Therefore, careful determination of A_f is necessary to get good results.

1.4 Factors affecting the hysteresis

The pseudoelastic hysteresis is affected by several factors, including strain rate, wire diameter, surface texture, and training of the wire.

1.4.1 Strain rate

The strain rate applied to a wire during a pseudoelastic cycle affects the material's response. As the strain rate $\dot{\epsilon}$ increases, it is expected that σ_{Ms} increases and σ_{As} decreases, resulting in a larger hysteresis. This is believed to be a result of the increase in internal friction as the driving force increases (Tobushi, Shimeno, Hachisuka, & Tanaka, 1998) (Grandi, Maraldi, & Molari, 2012). There is also an increase in residual strain upon unloading with increasing $\dot{\epsilon}$ (Tobushi, Shimeno, Hachisuka, & Tanaka, 1998). Another effect of strain rate is that at low

strain rates, an overshoot often occurs at σ_{Ms} that disappears at higher strain rates. For large wires, as $\dot{\epsilon}$ increases, the slope of the stress plateau during loading increases. This is because the M→A transition is exothermic, so heat is released upon loading. This causes the local temperature to rise, and thus the transition stress must rise, so the slope of the transition plateau increases until σ_{Mf} is reached. If $\dot{\epsilon}$ is high enough, the heat transfer coefficient of the material becomes immaterial and all wires, regardless of size, respond to the heat generation in the same way (Grandi, Maraldi, & Molari, 2012).

1.4.2 Wire diameter

Wire diameter, and thus grain size for oligocrystalline wires, affects the size of the pseudoelastic hysteresis. As the diameter decreases, hysteresis notably increases. This is mainly seen in wires with diameter D between 20-100 μm (Ueland & Schuh, 2012) (Chen & Schuh, 2011) (Lopez del Castillo, Mellor, Blazquez, & Gomez, 1987). In oligocrystalline wires, the grain spans the entire cross section so martensitic plates thicken along the length of the wire. As the wire gets thinner, there is a larger free surface area/volume ratio, which increases the frictional work and results in an increased σ_{Ms} (Ueland & Schuh, 2012). This reason also accounts for transformation temperatures that are inversely proportional to D (Chen & Schuh, 2011).

1.4.3 Surface texture

The surface texture affects the behavior of an oligocrystalline SMA wire because surface defects are a key place for cracks to develop, especially when fatigue must be considered.

Electropolishing the wires smooths the surface and reduces the number and intensity of stress concentrations. For Cu-based materials, it is recommended that they be electropolished in a 33% diluted phosphoric acid solution for 15-30 minutes with a voltage of 1.2-2.0 V and a current of 0.06-0.10 A/cm² (Davis & Associates, 2001).

1.4.4 Training

The first few pseudoelastic cycles a wire is subjected results in its being “trained.” Training allows for nucleation sites to form, initial propagation barriers to be overcome, and dislocations to form within the austenite phase that will encourage martensite formation. Because of this, after several cycles, both σ_{Ms} and σ_{As} decrease, with the former decreasing more quickly than the latter so the area within the total hysteresis get smaller with increasing cycling (Ueland & Schuh, 2012).

2. METHODOLOGY

2.1 Preparing wires

SMA wires were prepared using the Taylor liquid drawing technique, as described by Ueland and Schuh (Ueland & Schuh, 2012). Wires were drawn from solid pieces of compositions Cu-18%Al-10%Mn and Cu-25%Al-4%Mn-3%Ni. The solid metal pieces were inserted into borosilicate (Pyrex) glass tubes (working temperature 820°C), which were then subjected to vacuum conditions and refilled with low pressure argon. The tubes were then sealed by heating them over an oxyacetylene burner until the glass softened and the tube closed. Wires were formed by heating the metal inside the glass until the metal melted and the glass softened. Glass capillaries containing the molten metal were then drawn.

The glass-coated metal wires were heat treated to stabilize the β_1 austenite phase and promote growth of the bamboo structure. According to the phase diagram (see Figure 3), the wires required heat treatment above 800°C for this purpose. The drawn wires were placed in a quartz tube, subjected to vacuum conditions, and then refilled with a low pressure argon atmosphere before closing the tube. They were then annealed for 100-120 minutes at 900°C and subsequently water quenched. Figure 4 shows bamboo grain boundaries for two wires. The glass coating on the wires was removed by soaking them overnight in 10% diluted aqueous hydrofluoric acid.

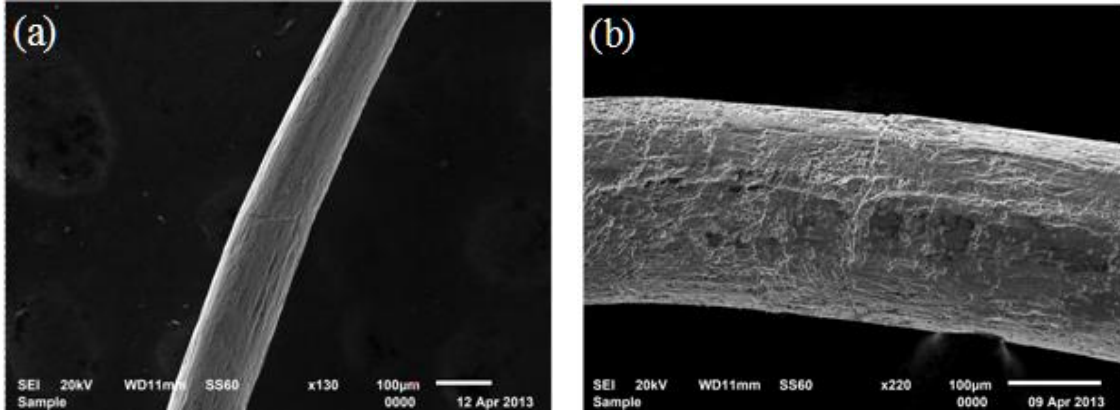


Figure 4. SEM images of (a) Wire C (after electropolishing) and (b) Wire F (as-pulled), showing the bamboo oligocrystalline structure.

Because surface texture has an effect on the pseudoelastic behavior of SMA wires, the wires were electropolished in a 33% diluted phosphoric acid aqueous solution. Polishing times ranged from 30 seconds to 90 minutes, and voltages from 1.5 volts to 3.5 volts. See Table 1 for details about each wire.

Table 1. Wire details, including composition, diameter, and polishing details.

Wire	Composition	Diameter (μm)	Electropolishing
A	Cu-18% Al-10% Mn	150	3V, 0.09A, 35s
B	Cu-25% Al-4% Mn-3% Ni	98	3V, 0.09A, 60s
C	Cu-25% Al-4% Mn-3% Ni	110	2.2V, 0.02A, 60min
D	Cu-25% Al-4% Mn-3% Ni	135	1.5V, 0.02A, 56min
E	Cu-25% Al-4% Mn-3% Ni	140	1.5V, 0.02A, 35min
F	Cu-25% Al-4% Mn-3% Ni	165	3.5V, 0.12A, 4min
G	Cu-25% Al-4% Mn-3% Ni	170	2.0V, 0.02A, 90min
H	Cu-25% Al-4% Mn-3% Ni	80	3.5V, 0.14A, 3min

2.2 Finding transformation temperatures

Pseudoelasticity tests must be run above A_f , so the transformation temperatures were found using a dynamic mechanical analyzer (DMA) equipped with a closed furnace (DMA Q800 from TA instruments). The wire ends were placed in mechanical grips in a plastic compound that were tightened to form a secure hold on the wire. A built-in high resolution linear optical encoder (nominal resolution: 1 nm) measured the cross-head displacement. To find the transformation temperature for the Cu-Al-Mn-Ni wires, constrained thermal cycling was performed on Wire B. A preload of 0.15 N (20 MPa) was applied and the temperature was cycled between 30 and 230°C at a rate of 4°C per minute. The results are shown in Figure 5.

Under these conditions, A_f was determined to be 126°C . From this data, and assuming a linear relationship between A_f and applied stress with slope of 2.5, A_f with no applied stress was determined to be 118°C . Therefore, pseudoelastic tests were run at or above 130°C so the wires would stay above A_f even while strained. The transformation temperatures found from Wire B are comparable to those found by Sari, whose results are in Table 2 (Sari, 2010).

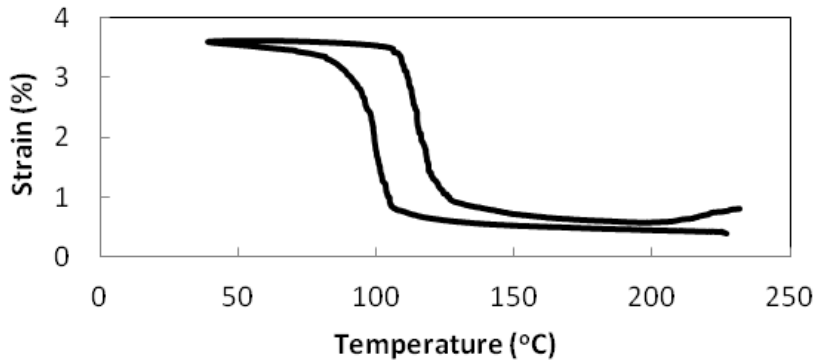


Figure 5. Thermal cycling data for Sample C at a constant load of 20 MPa.

Table 2. Compositions and transformation temperatures of the wires used by Sari (Sari, 2010).

Alloy	Chemical composition / wt%				Transformation temperature / °C			
	Cu	Al	Ni	Mn	Martensite finish, M_f	Martensite start, M_s	Austenite start, A_s	Austenite Finish, A_f
Cu-Al-Ni	84.3	11.9	3.8	—	222	235	230	263
Cu-Al-Ni-Mn	82	11.6	3.9	2.5	112	128	130	147

2.3 Testing pseudoelasticity

Pseudoelastic tests for Cu-Al-Mn wires were conducted isothermally at 40°C, as previous literature has shown that A_f is significantly below that (Koeda, et al., 2005). Cu-Al-Mn-Ni wire tests were conducted isothermally between 130°C and 140°C. The transition stresses were determined from the hysteresis by using a straight line approximation for the elastic and transformation regions and finding the intersection of these lines, as described by Tobushi, et. al (Tobushi, Shimeno, Hachisuka, & Tanaka, 1998). The data for the first few pseudoelastic cycles were not used unless further data was unable to be taken for a specific wire, as this reduced the influence of training the wire.

3. RESULTS AND DISCUSSION

3.1 Composition effects

The properties of both Cu-Al-Mn and Cu-Al-Mn-Ni wires were investigated. Figure 6 shows the beginnings of the hystereses of Wire A (Cu-Al-Mn) and Wire B (Cu-Al-Mn-Ni). For Wire A, σ_{Ms} was determined to be 52 MPa, and for Wire B, σ_{Ms} is 120 MPa. From this, it can be seen that the addition of Ni increases σ_{Ms} by a factor of two. Additionally, the Cu-Al-Mn wires that were tested never achieved a full hysteresis – they broke shortly after undergoing the M→A transformation. The Cu-Al-Mn-Ni wires, on the other hand, were able to achieve a full hysteresis with over 3% strain, which is over 1.5 times than the 2% that Sutou, et. al., found for Cu-Al-Mn (Sutou, Omori, Kainuma, Ono, & Ishida, 2002).

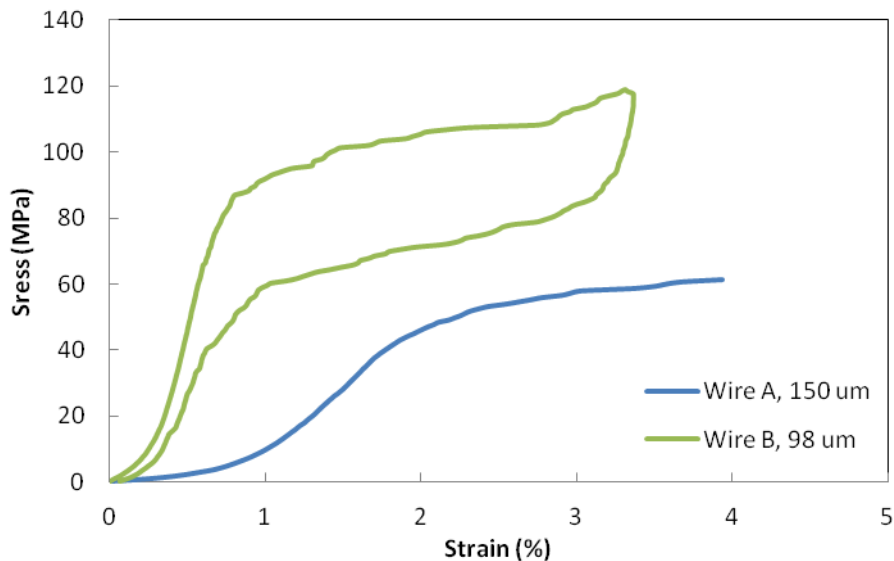


Figure 6. Pseudoelastic hystereses for Wire A (Cu-Al-Mn) and Wire B (Cu-Al-Mn-Ni).

3.2 Strain rate effects

Figure 7 shows the hystereses of Wire B at varying loading rates at 130°C. A constant load method was used for this research, instead of constant strain as is commonly found in the literature, but the expected qualitative results should be comparable. Specifically, as the loading rate increases, σ_{Ms} decreases while σ_{As} increases, thus resulting in a decrease in the size of the hysteresis (Tobushi, Shimeno, Hachisuka, & Tanaka, 1998). However, this was found not to be the case. Figure 7 shows the hystereses of Wire B responding to various load rates, ranging from 5 MPa/min to 40 MPa/min. As this figure and Table 3. Transformation stresses σ_{Ms} and σ_{As} for Wire B (D=98 μ m) for various load rates. portray, increasing the loading rate decreased the size of the hysteresis by decreasing σ_{Ms} and increasing σ_{As} .

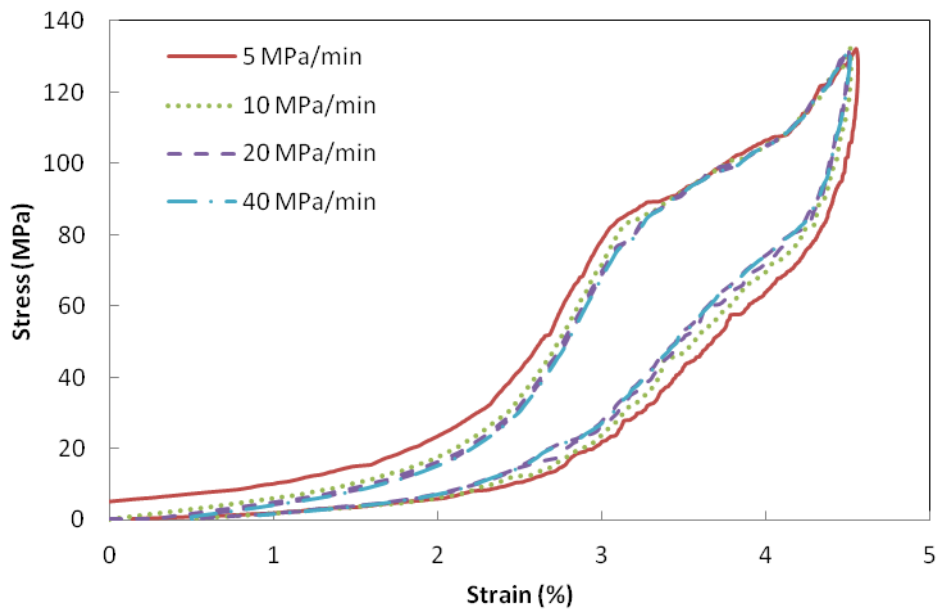


Figure 7. Pseudoelastic hysteresis for Wire B (D=98 μ m) at various strain rates.

Table 3. Transformation stresses σ_{Ms} and σ_{As} for Wire B (D=98 μ m) for various load rates.

Load Rate (MPa/min)	σ_{Ms} (MPa)	σ_{As} (MPa)
5	84	79
10	82	84
20	81	87
40	81	87

This may be a result of several factors. First, the wires may not have had sufficient training. Training wires reduces σ_{Ms} because the material's microstructure has already gone through the transformation, so there are nucleation sites and other defects already present that promote martensite plate growth. Thus σ_{Ms} may have been increasing for larger rates, but due to the lack of training, this behavior wasn't seen.

Additionally, because a constant load rate was used, not a constant strain rate, the strain rate decreased as the load neared its maximum value. This may mean that the slowing of the elongation increased the time for the phase transformation to occur and thus the wire was able to equilibrate easier with regards to the competition between the driving force (external stress) and the barrier to transformation (temperature). Thus because it could equilibrate more easily, a higher driving force wasn't needed to begin the martensitic transformation. More tests on other wires are needed to support or refute these hypotheses.

3.3 Wire diameter effects

There was no correlation found between wire diameter, and thus grain size for bamboo-structured wires, and the transformation stresses. The pseudoelastic hystereses for Wires B through G ($D = 98\text{-}170\ \mu\text{m}$) are depicted in Figure 8. Figure 9 shows graphically σ_{Ms} for the wires based on their diameter. This graph clearly shows the lack of correlation between diameter and σ_{Ms} .

These results were expected, based on previous studies found in the literature. Chen and Schuh determined that the critical grain size is approximately $100\ \mu\text{m}$, where wires larger than this have similar responses regardless of size (Chen & Schuh, 2011). As all of the wires tested were $\geq \sim 100\ \mu\text{m}$ in diameter, no correlation between grain size and transformation temperature matches the literature well.

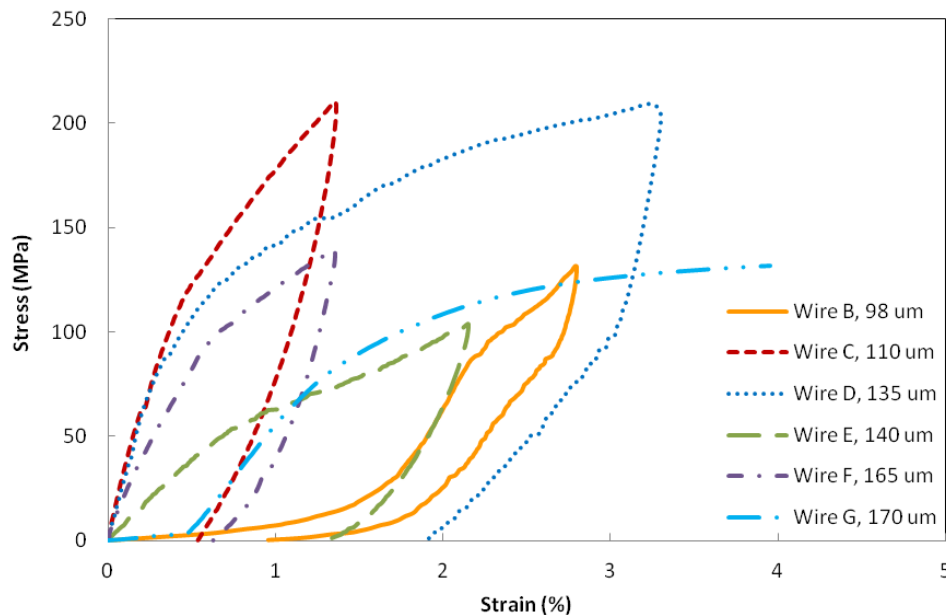


Figure 8. Pseudoelastic hystereses for Cu-Al-Mn-Ni wires with diameters ranging from $98\text{-}170\ \mu\text{m}$.

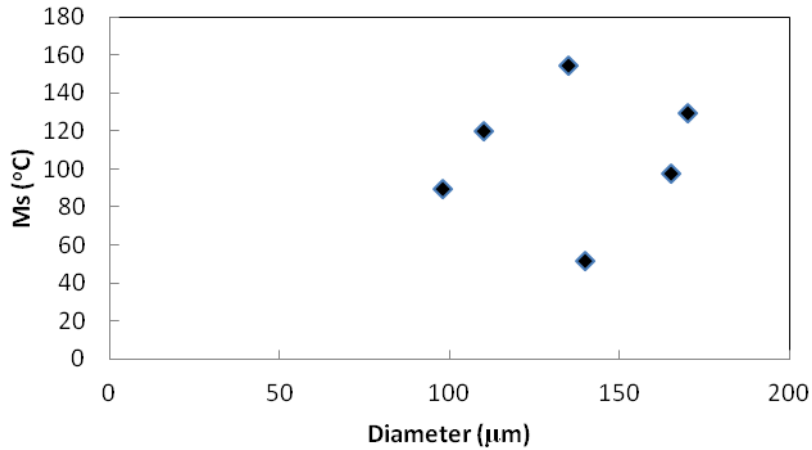


Figure 9. Relationship between martensitic transformation stress σ_{M_s} and wire diameter D for Wires B through G.

3.4 Surface texture effects

Because triple junctions are a significant cause of failure, electropolishing the wires to reduce stress concentrators can improve the quality of the pseudoelastic hysteresis as well as other SME properties. Figure 10 shows SEM micrographs of Wire F before and after electropolishing. The polishing smoothes the surface and more clearly shows the bamboo grain boundaries. Wire F was polished for four minutes at 3.5 V and 0.12 A.

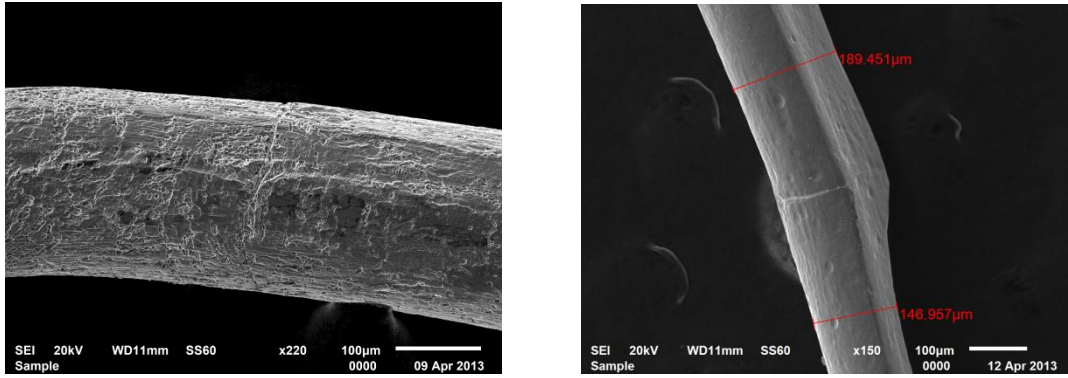


Figure 10. SEM images of Wire F as-pulled and after electropolishing (3.5 V, 0.12 A, 4 min).

However, too much polishing can be problematic, as shown in Figure 11. Wire H was polished for three minutes at 3.5 V and 0.14 A. The wire was preferentially etched so the resulting surface had much greater dimples than the as-drawn wire. The voltage, current, and time of polishing is dependent on the surface area of the wire. Wires F and H had almost identical polishing conditions, but because Wire H had a diameter half that of Wire F, Wire H was overpolished while Wire F was polished well.

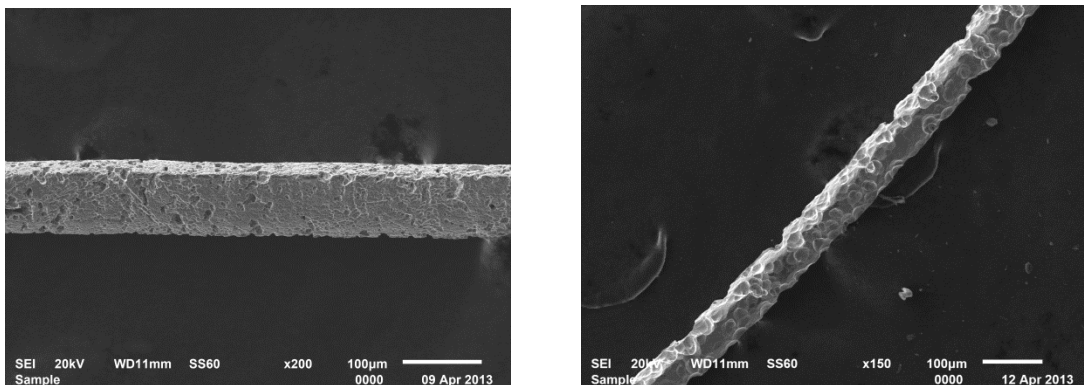


Figure 11. SEM images of Wire H as-pulled and after electropolishing (3.5 V, 0.14 A, 3 min).

4. CONCLUSION

Shape memory alloys have many properties that make them useful materials in a variety of applications. The abilities to change shape when heat or stress is applied and recover the initial shape after absorbing considerable amounts of energy are just two of these properties. However, the Ni-Ti alloys that are currently used are expensive and can only be used at ambient temperatures. Therefore, there must be research on new SMAs that can improve these properties.

This research focused on a Cu-Al-Mn-Ni alloy as a potential alternative. The response of the pseudoelastic behavior of oligocrystalline wires was investigated in response to various conditions, including strain rate, wire diameter, and surface texture. It was found that the pseudoelastic hysteresis decreases with respect to increasing strain rate. The pseudoelastic hysteresis showed no correlation to wire diameter, as has also previously been confirmed in the literature. Additionally, although no quantitative conclusions could be drawn from the data, it was observed that surface texture does play a role in the behavior of the wires. The smoother the surface, the better SME the wires exhibited. From this, it can be concluded that with the right surface texture, Cu-Al-Mn-Ni oligocrystalline wires are a good candidate for SMA applications.

5. FUTURE WORK

This research has brought up several questions to be investigated further. For one, it was shown that Cu-Al-Mn wires have considerably worse properties than Cu-Al-Mn-Ni wires. However, it has been shown in the literature that Cu-Al-Mn alloys do work with the proper composition and heat treatment to ensure the best microstructure (Sutou, Omori, Kainuma, Ono, & Ishida, 2002) (Lopez del Castillo, Mellor, Blazquez, & Gomez, 1987) (Koeda, et al., 2005). Thus one direction of future research is to determine the appropriate processing methods to see if this alloy is viable.

Additionally, one of the reasons why some of the wires may not have shown perfect hystereses and broke after few cycles is that they may not have had a perfect bamboo structure. The presence of triple junctions decreases the strength of the material significantly. Thus another direction of future research is to investigate the effect of heat treatment on the wire microstructure, such as through temperature and time.

Finally, as seen in Section 3.4 Surface texture effects, surface texture has an effect on the SM ability of the wires. Too little surface polishing can leave stress concentrations, while too much polishing can lead to preferential removal of material, thus causing greater surface defects than originally present. Thus future research may be devoted to determining the optimal electropolishing conditions, including voltage, current, and time.

6. ACKNOWLEDGEMENTS

I would like to thank Nihan Tuncer, who helped to develop the idea for and implement this research, and who guided me through the whole process. Additional thanks goes to Professor Christopher Schuh, my advisor, and the rest of the Schuh research group for introducing me to their research and offering their assistance. I would also like to acknowledge David Bono for his help with imaging the wires. This research was supported by the Institute for Soldier Nanotechnologies at MIT.

7. BIBLIOGRAPHY

Chen, Q. F., Zuo, X. B., Wang, L. M., Chang, W., Tian, W. Y., Li, A. Q., et al. (2006). NiTi wire as a superelastic damping material in structural engineering. *Materials Science and Engineering A* , 438-449, 1089-1092.

Chen, Y., & Schuh, C. A. (2011). Size effects in shape memory alloy microwires. *Acta Materialia* , 59, 537-553.

Davis & Associates. (2001). *Copper and Copper Alloys*. (J. R. Davis, Ed.) Materials Park, OH: ASM International.

Grandi, D., Maraldi, M., & Molari, L. (2012). A microscale phase-field model for shape memory alloys with non-isothermal effects: Influence of strain rate and environmental conditions on the mechanical response. *Acta Materialia* , 60, 179-191.

Koeda, N., Omori, T., Sutou, Y., Suzuki, H., Wakita, M., Kainuma, R., et al. (2005). Damping properties of ductile Cu-Al-Mn-based shape memory alloys. *Materials Transactions* , 46, 118=122.

Lopez del Castillo, C., Mellor, B. G., Blazquez, M. L., & Gomez, C. (1987). The influence of composition and grain size on the martensitic transformation temperatures of Cu-Al-Mn shape memory alloys. *Scripta Metallurgica* , 21, 1711-1716.

Omori, T., Koeda, N., Sutou, Y., Kainuma, R., & Ishida, K. (2007). Superplasticity of Cu-Al-Mn-Ni Shape Memory Alloy. *Materials Transactions* , 48 (11), 2914-2918.

Otuska, K., Wayman, C. M., Nakai, K., Sakamoto, H., & Shimizu, K. (1976). Superelasticity effects and stress-induced martensitic transformations in Cu-Al-Ni alloys. *Acta Metallurgica* , 24, 207-226.

Ren, C.-c., Bai, Y.-x., Wang, H.-m., Zheng, Y.-f., & Li, S. (2008). Phase transformation analysis of varied nickel-titanium orthodontic wires. *Chinese Medical Journal* , 121 (20), 2060-2064.

Sakamoto, H., Kijima, Y., & Shimizu, K. (1982). Fatigue and fracture characteristics of polycrystalline Cu-Al-Ni shape memory alloys. *Transactions of the Japan Institute of Metals* , 23 (10), 585-594.

Sari, U. (2010). Influences of 2.5wt% Mn addition on the microstructure and mechanical properties of Cu-Al-Ni shape memory alloys. *International Journal of Minerals, Metallurgy and Materials* , 17 (2), 192-198.

Sutou, Y., Omori, T., Kainuma, R., Ono, N., & Ishida, K. (2002). Enhancement of superelasticity in Cu-Al-Mn-Ni shape memory alloys by texture control. *Metallurgical and Materials Transactions A* , 33A, 2817-2824.

Tobushi, H., Shimeno, Y., Hachisuka, T., & Tanaka, K. (1998). Influence of strain rate on superelastic properties of TiNi shape memory alloy. *Mechanics of Materials* , 30, 141-150.

Ueland, S. M., & Schuh, C. A. (2012). Superelasticity and fatigue in oligocrystalline shape memory alloy microwires. *Acta Materialia* , 60, 282-292.

Ueland, S. M., Chen, Y., & Schuh, C. A. (2012). Oligocrystalline shape memory alloys. *Advanced Functional Materials* , 22, 2094-2099.

Zhang, X., Feng, P., He, Y., Yu, T., & Sun, Q. (2010). Experimental study on rate dependence of macroscopic domain and stress hysteresis in NiTi shape memory alloy strips. *International Journal of Mechanical Sciences* , 52, 1660-1670.